Geophysical Journal International

Geophys. J. Int. (2020) **223,** 612–621
Advance Access publication 2020 June 27
GJI Seismology

doi: 10.1093/gji/ggaa324

Constraining 1-D inner core attenuation through measurements of strongly coupled normal mode pairs

S. Talavera-Soza and A. Deuss

Department of Earth Sciences, Utrecht University, Princetonlaan 8A, Utrecht 3584CB, Netherlands. *E-mail: s.a.talaverasoza@uu.nl*

Accepted 2020 June 16. Received 2020 May 11; in original form 2020 January 21

SUMMARY

We measured inner core normal mode pair ${}_{10}S_2$–${}_{11}S_2$, which cross-couples strongly for 1-D structure and is sensitive to shear wave velocity, and find that our measurements agree with a strongly attenuating inner core. In the past, this mode pair has been used to try to resolve the debate on whether the inner core is strongly or weakly attenuating. Its large spectral amplitude in observed data, possible through the apparent low attenuation of ${}_{10}S_2$, has been explained as evidence of a weakly attenuating inner core. However, this contradicted body waves and other normal modes studies, which resulted in this pair of modes being excluded from inner core modelling. Modes ${}_{10}S_2$ and ${}_{11}S_2$ are difficult to measure and interpret because they depend strongly on the underlying 1-D model used. This strong dependence makes these modes change both their oscillation characteristics and attenuation values under a small 1-D perturbation to the inner core model. Here, we include this effect by allowing the pair of modes to cross-couple or resonate through 1-D structure and treat them as one hybrid mode. We find that, unlike previously thought, the source of ${}_{10}S_2$ visibility is its strong cross-coupling to ${}_{11}S_2$ for both 1-D elastic and anelastic structure. We also observe that the required 1-D perturbation is much smaller than the 2 per cent v_s perturbation previously suggested, because we simultaneously measure 3-D structure in addition to 1-D structure. Only a 0.5 per cent increase in inner core v_s or a 0.5 per cent decrease in inner core radius is required to explain ${}_{10}S_2$–${}_{11}S_2$ observations and a weakly attenuating inner core is not needed. In addition, the 3-D structure measurements of mode ${}_{10}S_2$ and its cross-coupling to ${}_{11}S_2$ show the typical strong zonal splitting pattern attributed to inner core cylindrical anisotropy, allowing us to add further constrains to deeper regions of the inner core.

Key words: Core; Seismic anisotropy; Seismic attenuation; Surface waves and free oscillations; Theoretical seismology.

1 INTRODUCTION

Inner core solidity was first observed using whole Earth oscillations or normal modes by Dziewonski & Gilbert (1971), although it had already been predicted by a number of authors (i.e. Lehmann 1936; Birch 1940; Bullen 1946) before any direct observations were available. Additional evidence came some three decades later from inner core shear wave measurements, or PKJKP (Deuss *et al.* 2000; Cao *et al.* 2005; Wookey & Helffrich 2008; Tkalčić & Pham 2018). Currently, inner core solidity together with its shear wave velocity of $v_s = 3.6$ km s^{-1}, are widely accepted.

However, inner core intrinsic attenuation, or absorption of energy as waves travel through Earth, still remains an outstanding problem. The main issue is the incompatibility between body waves and normal modes based models of shear attenuation Q_μ. Early normal modes studies proposed a weakly attenuating inner core with $Q_\mu >$ 1000, based on modes sensitive to v_s in the whole inner core, while body waves studies inferred a strongly attenuating inner core with $Q_\mu \sim 40$, by assuming no significant bulk attenuation or frequency dependence and mainly constraining the top 500 km of the inner core (Romanowicz & Mitchell 2007). The Preliminary Reference Earth Model (PREM, Dziewonski & Anderson 1981), which was created using a combination of both normal mode and body wave data, has a strongly attenuating inner core with $Q_\mu = 84$ and has non-zero bulk attenuation with $Q_\kappa = 1328$ mostly constrained using radial modes. More recent normal modes studies, based on modes sensitive to v_p in the shallower and deeper inner core, are also in favour of a strongly attenuating inner core (Widmer *et al.* 1991; Durek & Ekström 1995; Resovsky *et al.* 2005; de Wit *et al.* 2014), with $Q_\mu = 90$–110. Nevertheless, body waves still prefer an even more strongly attenuating inner core than normal modes. Two possibilities have been suggested to overcome the disagreement either (i) non-zero inner core bulk attenuation Q_κ in order to explain strong compressional wave attenuation, or (ii) frequency dependent Q_μ in

order to explain stronger attenuation at high body wave frequencies than at low normal mode frequencies. Unfortunately, no consensus has yet been reached, as even the widely used assumption of shear attenuation dominating over bulk attenuation has now been questioned (Morozov 2015), since it leads to auxetic elastic materials, which have a negative Poisson's ratio and are extremely rare in nature.

In the past, the mode pair ${}_{10}S_2$–${}_{11}S_2$ has been used to try to resolve the debate on inner core attenuation. In PREM, both modes are mainly inner core confined and have such a low Q (i.e. strong attenuation) that their synthetic spectral amplitudes are more than 100 times smaller than observed earthquake data, rendering them invisible in synthetic normal mode spectra. This does not agree with the real data, where a large peak is visible (see Fig. 1). Modes ${}_{10}S_2$ and ${}_{11}S_2$ depend strongly on the underlying 1-D model used, changing their oscillation characteristics under small changes to inner core 1-D structure (Andrews *et al.* 2006). Because of this, the discussion about these modes concentrates on what their large amplitudes and their corresponding Q values indicate for inner core attenuation structure.

The centre frequencies f_c and Q values, which describe attenuation, of ${}_{10}S_2$ and ${}_{11}S_2$ were first measured by Dziewonski & Gilbert (1973). They identified two peaks in the data and proposed two possible explanations for them: (i) either only ${}_{10}S_2$ is visible and strongly split or (ii) both modes have visible peaks in the data without significant splitting. They preferred the latter explanation, as at the time no other strongly split inner core sensitive modes had been measured. They also concluded that to make ${}_{11}S_2$ visible, the inner core had to be weakly attenuating.

Later, after numerous strongly split inner core sensitive modes were identified, Masters & Gilbert (1981) proposed instead that the source of both peaks was the strong splitting of ${}_{10}S_2$, and interpreted the large amplitude peak of ${}_{10}S_2$ again as proof of a weakly attenuating inner core ($Q = 1079$, Masters & Gilbert 1983). This contradicted short period body wave observations, suggesting a frequency dependent Q_μ (Cormier 1981; Doornbos 1983; Li & Cormier 2002). Ritzwoller *et al.* (1986) confirmed that ${}_{10}S_2$ is strongly split, by comparing non-polar stations, where they observed two peaks, and polar stations, where they only identified one peak corresponding to ${}_{10}S_2$. Shortly after, Giardini *et al.* (1988) measured a Q value of 800 for ${}_{10}S_2$, and highlighted the importance of its 1-D cross-coupling to ${}_{11}S_2$ when measuring its splitting, in order to include the strong 1-D model dependance of ${}_{10}S_2$ and ${}_{11}S_2$. Later papers questioned again the observation of ${}_{11}S_2$ and other inner core confined modes (Masters & Shearer 1990), which prompted the exclusion of these modes in further Q_μ modelling (i.e. Widmer *et al.* 1991). As a consequence, modes ${}_{10}S_2$–${}_{11}S_2$ have been excluded in the last few decades from other comprehensive normal mode measurements (i.e. He & Tromp 1996; Resovsky & Ritzwoller 1998; Deuss *et al.* 2013).

More recently, synthetic tests performed by Andrews *et al.* (2006) confirmed that, in order to take into account the strong 1-D model dependance of ${}_{10}S_2$–${}_{11}S_2$, 1-D cross-coupling must be included when using perturbation theory to calculate synthetic spectra. They found that indeed the source of ${}_{10}S_2$ high Q is its strong cross-coupling to ${}_{11}S_2$ for 1-D structure. Just like Giardini *et al.* (1988), they point out that in PREM both modes are a mix of PKIKP equivalent mode and inner core confined oscillation, but that a small perturbation to the 1-D model will change ${}_{10}S_2$ and ${}_{11}S_2$ mode identities. To include this effect in their synthetics, they combined a 2 per cent v_s perturbation to the inner core with 1-D Q cross-coupling. Their results had the same effect as recalculating the mode catalogue with a 2 per cent v_s change in the 1-D model: one of the modes increased its Q value more than five times to become PKIKP equivalent, while the other mode decreased its Q to become almost completely inner core confined. As a consequence, their synthetic spectra of ${}_{10}S_2$–${}_{11}S_2$ now had amplitudes comparable to the real data. The Q values changes in these modes are entirely due to the variations in inner core v_s, while keeping the inner core strongly attenuating ($Q_\mu = 84$). They showed that their results for ${}_{10}S_2$ and ${}_{11}S_2$ can be obtained using either (i) perturbation theory, including higher order 1-D Q coupling or (ii) by recalculating the mode catalogue (Woodhouse 1988), with both methods giving identical results. While Andrews *et al.* (2006) only explored the effect of v_s on modes ${}_{10}S_2$–${}_{11}S_2$, 1-D variations to the inner core radius have also been proposed to have a similar effect (Widmer 2002). Here, we will explore the effect of both parameters.

In this paper, we measure ${}_{10}S_2$–${}_{11}S_2$ and confirm that ${}_{10}S_2$ indeed becomes visible through higher order 1-D Q cross-coupling. Like in previous studies, we also observe two peaks, which we confirm is due to strong splitting of ${}_{10}S_2$ and is not ${}_{11}S_2$, which we agree is invisible. In addition, we show that the source of the visibility of ${}_{10}S_2$ in real data is indeed due a 1-D perturbation in inner core v_s or radius, and not a weakly attenuating inner core. We also apply the same analysis to mode pair ${}_8S_2$–${}_9S_2$, which cross-couples for 1-D v_p structure. Finally, we use our new measurements for the centre frequency and Q values to determine the amount of change in inner core v_s or radius required to explain our observations.

2 THEORY

Normal modes are standing waves along the radius and surface of our planet, that only exist for discrete frequencies. In this study, we will concentrate on spheroidal modes, which consist of P–SV motion. Spheroidal modes ${}_nS_l$ are characterized by two numbers, the angular order l and the overtone number n. Each mode with a given l is a multiplet consisting of $2l + 1$ singlets. In a spherical, non-rotating, elastic, isotropic Earth, these $2l + 1$ singlets are degenerate, meaning they all have the same frequency. The degeneracy is removed by the effects of rotation, ellipticity, anisotropy and lateral heterogeneities, which we call splitting. We calculate splitting through perturbation theory (Dahlen 1968; Woodhouse & Dahlen 1978; Woodhouse 1980). This calculation can either be in the self-coupling approximation, where modes are treated as isolated; group-coupling, which includes the cross-coupling between a pair or small group of modes close in frequency; or full-coupling, were cross-coupling between all modes in a certain frequency band is included (e.g. Deuss & Woodhouse 2001). In self-coupling, a mode is sensitive to structure of degree $s = 2l$. In cross-coupling, two spheroidal modes, with angular orders l and l', are sensitive to $|l - l'| \leq s \leq |l + l'|$ structure.

We concentrate on mode pairs ${}_nS_l$-${}_{n'}S_{l'}$ with $l = l'$ and $n = n' \pm 1$. These rare occurring pairs are sensitive to 1-D structure (i.e. $s = 0$), with modes ${}_{n\pm1}S_2$-${}_nS_2$ coupling for degrees $s = 0, 2, 4$. For these mode pairs, degree-zero or 1-D cross-coupling is significantly strong, and by fully including it we obtain the same results using perturbation theory as recalculating the normal mode catalogue. For details, see (Andrews *et al.* 2006). Here, full-coupling with additional modes is considered a second order effect.

We use the generalized splitting function approach (Resovsky & Ritzwoller 1998) to measure normal mode splitting for a pair of strongly coupled modes. Splitting functions are depth-averaged models of how one particular mode 'sees' the Earth (Woodhouse &

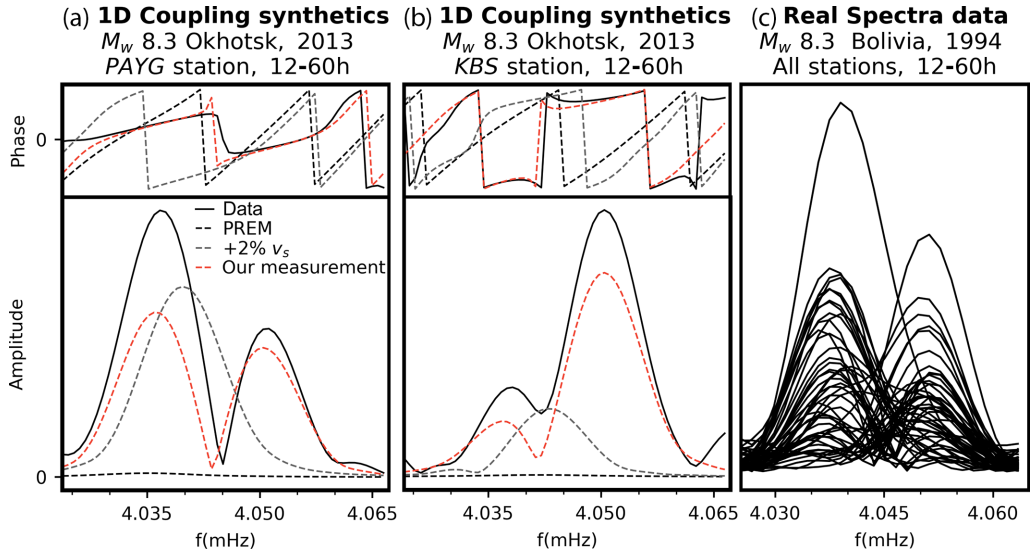

Figure 1. Observed data (solid black line) and synthetics for ${}_{10}S_2$–${}_{11}S_2$: (a) station PAYG located in the Galapagos Islands, and (b) station KBS located in Svalbard, Norway. Both stations are from the 2013 Okhotsk event. Synthetics are calculated for PREM (black dashed line), a 2 % inner core v_s increase (grey dashed line) and using our measurements of their splitting function coefficients (red dashed line). Also shown are (c) all observed spectra used for the 1994 Bolivia event. Although not shown, a 2 % inner core radius decrease has a similar behaviour on the spectra as a 2 % v_s increase.

Giardini 1985), their coefficients are written as

$$c_{st}^{kk'} = \int_0^a \delta m_{st}(r) \cdot K_s^{kk'}(r)\,\mathrm{d}r + \sum_d \delta h_{st}^d\, H_s^{d,\,kk'}, \tag{1}$$

where s is the angular order and t the azimuthal order of the Earth's structure, and the integral is calculated over a, the radius of the Earth. $K_s^{kk'}$ and $H_s^{d,\,kk'}$ are known kernels (Woodhouse 1980), with $k = (l, m)$ for mode 1 and $k = (l', m')$ for mode 2; δm_{st} are the coefficients of the Earth's structure (compressional and shear wave velocity v_p, v_s; density ρ) and δh_{st}^d are the coefficients of discontinuity topography. For a pair of cross-coupling modes, three splitting functions will be measured jointly: self-coupling for mode 1 with kk, self-coupling for mode 2 with $k'k'$, and cross-coupling for modes 1 and 2 with kk'. Splitting function coefficients can be visualized in a map $F(\theta, \phi)$, that shows the regional frequency variations for a specific normal mode, that is,

$$F(\theta, \phi) = \sum_{s=2}^{2l} \sum_{t=-s}^{s} Y_s^t(\theta, \phi)\, c_{st}, \tag{2}$$

where $Y_s^t(\theta, \phi)$ are the fully normalized complex spherical harmonics and (θ, ϕ) indicate the surface position (Edmonds 1960). The degree-zero (c_{00}) elastic and anelastic coefficients of a self-coupled splitting function allow us to calculate the observed f_c and Q of a mode with respect to PREM.

$$f_c = f_0 + (4\pi)^{-1/2}\,\mathrm{Re}(c_{00}) \tag{3}$$

$$Q = \frac{f_c}{2\left(\frac{f_0}{2Q_0} + (4\pi)^{-1/2}\,\mathrm{Im}(c_{00})\right)}. \tag{4}$$

Here, we exclusively study mode pairs ${}_{n\pm1}S_2$–${}_nS_2$ that cross-couple strongly for 1-D structure (Andrews *et al.* 2006). These pairs become a hybrid multiplet, as their apparent f_c and Q values are greatly influenced by the degree-zero elastic and anelastic coefficients of their associated cross-coupled splitting function. This effect is excluded when f_c and Q are calculated using eqs (3) and (4). Thus, we report two different f_c and Q values for these modes: (i) the f_c and Q with respect to PREM, calculated using eqs (3) and (4), which can be interpreted with PREM's sensitivity kernels and used to model inner core structure and (ii) the hybrid multiplet f_c^h and Q^h values calculated directly from their splitting matrix with the diagonal sum rule (Gilbert 1971), which should not be used to model inner core structure with PREM's sensitivity kernels.

3 METHOD AND DATA

We invert for the splitting function coefficients for mode pairs using iterated least-squares (Tarantola & Valette 1982), following the same methodology as Deuss *et al.* (2013). As a large 1-D perturbation is necessary to make modes ${}_{10}S_2$–${}_{11}S_2$ visible in the spectra, we test a range of c_{00} coefficients for the starting model of these modes and their cross-coupling, which encompass any potential 1-D perturbation (i.e. v_s, v_p, ρ, radius) as seen in eq. (1). The reported uncertainties of the c_{00} coefficients of ${}_{10}S_2$–${}_{11}S_2$ were calculated based on the range of starting models that generated similar results.

Modes ${}_{10}S_2$–${}_{11}S_2$ and ${}_8S_2$–${}_9S_2$ are inner core sensitive modes, so we also need to take inner core anisotropy into account (e.g. Woodhouse *et al.* 1986). Inner core anisotropy with cylindrical symmetry leads to anomalously large values of the zonal coefficients, c_{20} and c_{40}. Current inner core anisotropy models overpredict these values or have contradictory predictions for ${}_{10}S_2$ and ${}_{11}S_2$. We try a range of c_{20} values to test the best starting models, as it is usually not possible for inner core sensitive modes to converge to a solution by just starting from PREM, while all our c_{40} coefficients are started from PREM. We also include mantle predictions for comparison to our observations, which are computed using v_s model S20RTS (Ritsema *et al.* 1999), with scaling of the form $\delta v_p/v_p = 0.5\,\delta v_s/v_s$ and $\delta\rho/\rho = 0.3\,\delta v_s/v_s$, together with crustal structure model CRUST5.1 (Mooney *et al.* 1998).

We use Deuss *et al.* (2013) and Koelemeijer *et al.* (2013) catalogue of events, and add the 2013 M_w 8.3 Sea of Okhotsk earthquake at 611 km depth. The starting catalogue contains 93 events, but we use a smaller subset which mainly includes deep earthquakes, as they are better at exciting inner core sensitive modes (Table 1).

Table 1. f_c and Q measurements with respect to PREM and apparent f_c^h and Q^h values of the hybrid multiplet, compared to PREM's. Misfits for: PREM (m^P), S20RTS with CRUST5.1 (m^{S20}) and our measurements (m^{cst}). N_{ev} number of events, N_s number of stations used.

	f_0	f_c	f_c^h	Q_0	Q	Q^h	m^P	m^{S20}	m^{cst}	N_{ev}	N_s
${}_8S_2$	3214.23	$3213.83^{+0.10}_{-0.02}$	3214.46	339	270^{+5}_{-3}	267	0.70	0.91	0.34	57	740
${}_9S_2$	3231.75	$3230.72^{+0.18}_{-0.08}$	3230.78	407	432^{+15}_{-5}	431					
${}_{10}S_2$	4032.33	$4043.62^{+2.82}_{-2.82}$	4040.09	192	211^{+31}_{-1}	670	0.97	0.98	0.35	58	1320
${}_{11}S_2$	4058.47	$4069.49^{+2.82}_{-2.82}$	4073.11	131	135^{+1}_{-5}	95					

4 RESULTS

We have measured splitting functions and corresponding f_c and Q values for mode pairs ${}_{10}S_2$–${}_{11}S_2$ and ${}_8S_2$–${}_9S_2$, taking all cross-coupling within each mode pair into account. Modes ${}_{10}S_2$ and ${}_{11}S_2$ are strongly dependent on the 1-D model used and are mostly sensitive to v_s in the inner core. Their frequencies are very similar in PREM, 4.032 mHz for ${}_{10}S_2$ and 4.058 mHz for ${}_{11}S_2$, making them appear almost on top of each other and therefore cross-coupling strongly. They are isolated from nearby modes and thus can be measured as a pair ignoring further cross-coupling. PREM also predicts similar sensitivity kernels and Q values, that is 192 for ${}_{10}S_2$ and 131 for ${}_{11}S_2$. In PREM, both modes are almost inner core confined and their extremely low Q values make them nearly invisible in its calculated synthetic spectra, however a small change to PREM's 1-D inner core structure can change the modes oscillation characteristics (Figs 1a and b).

Other mode pairs, of the type ${}_{n\pm1}S_l$-${}_nS_l$, have very different Q values, with one mode always being completely inner core confined and with a much lower Q than the other mode. The modes in these other pairs are more separated in frequency and usually overlaid by additional modes, which makes it more complicated to measure their splitting functions. Only ${}_8S_2$ and ${}_9S_2$ are close enough in frequency to be also measured as a pair. Like ${}_{10}S_2$–${}_{11}S_2$, the pair is sensitive to the inner core and couples for 1-D structure. Contrary to ${}_{10}S_2$–${}_{11}S_2$, ${}_8S_2$–${}_9S_2$ is also sensitive to the mantle and mostly to v_p instead of v_s.

4.1 ${}_{10}S_2$–${}_{11}S_2$

The presence of ${}_{10}S_2$–${}_{11}S_2$ in the real data (Fig. 1) provides constraints on inner core shear wave velocity, radius and Q. PREM predicts such low Q values for both modes that they are invisible in synthetic spectra when compared to real data. Andrews *et al.* (2006) showed that mode pair ${}_{10}S_2$–${}_{11}S_2$ is strongly dependent on small changes in the underlying 1-D model used. A peak becomes visible and comparable to the real data only by changing PREM's inner core v_s by 2 per cent and keeping inner core Q_μ at PREM values of 84 (Figs 1a and b). Unlike mode pairs dominated by rotation cross-coupling, which result in the Q values of the two modes to become more similar, a 2 per cent v_s increase leads ${}_{10}S_2$ to become a PKIKP equivalent mode with $Q = 706$, sensitive to both the mantle and the inner core, and ${}_{11}S_2$ to become an inner core confined mode with $Q = 91$ (Fig. 2). The opposite happens when v_s decreases by 2 per cent. Similarly, decreasing the inner core radius R by 2 per cent has the same effect as a 2 per cent v_s increase and vice versa. The same outcome can be obtained by either recalculating the mode catalogue using MINEOS, or by using perturbation theory including 1-D cross-coupling between these modes (Fig. 2b). Excluding 1-D cross-coupling prompts the Q of both modes to remain quite similar and close to PREM (Fig. 2a). For example, if no v_s perturbation is present, and only cross-coupling due to rotation and ellipticity is included, then only one of the singlets of ${}_{10}S_2$ increases its Q value to 800 (Fig. 2b), which is not enough to produce an amplitude peak comparable to the observed spectra (Figs 1a and b).

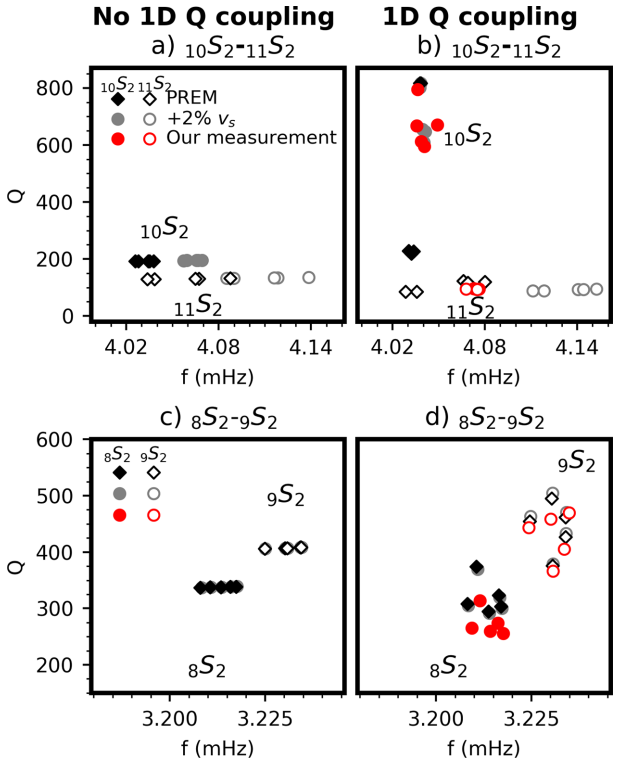

Figure 2. Normal mode singlet Q values versus frequencies for: PREM, a 2 % inner core v_s increase, and our measurements. All include the effects of rotation and ellipticity. Values are shown for modes ${}_{10}S_2$–${}_{11}S_2$ and ${}_8S_2$–${}_9S_2$: (a, c) without 1-D cross-coupling and (b, d) with 1-D cross-coupling. Although not shown, a 2 % inner core radius decrease has a similar behaviour on the modes singlets as a 2 % v_s increase. The measured singlets of ${}_{10}S_2$ and ${}_{11}S_2$ are listed in Table 2.

Table 2 Singlet frequencies and Q values for our measurement of modes ${}_{10}S_2$–${}_{11}S_2$ in Fig 2(b).

	f	Q
${}_{10}S_2$	4049.05	671
	4035.81	667
	4036.37	794
	4038.59	612
	4040.56	596
${}_{11}S_2$	4067.79	94
	4076.15	95
	4074.96	93
	4072.64	97
	4073.98	95

It is important to note that these changes are due to the c_{00} values varying, which can also be due to changes in v_p and density, instead of v_s or inner core radius. Thus, we measured ${}_{10}S_2$–${}_{11}S_2$ starting from a range of positive and a negative c_{00} values, and obtained stable results in both cases. Starting from a positive c_{00} perturbation results in a lower misfit (0.35) and requires a much smaller deviation from PREM, with ${}_{10}S_2$ becoming the observable mode. Alternatively, starting from a negative c_{00} perturbation leads to a larger misfit (0.46), and the need for a much larger deviation from PREM to make ${}_{11}S_2$ observable. This larger deviation from PREM stems from ${}_{11}S_2$ being predicted to appear further away from the peak seen in the real data. Based on our measurements and synthetics calculations, we conclude that the best possible solution is that starting from a positive c_{00} value for ${}_{10}S_2$ and ${}_{11}S_2$. Positive c_{00} values could be due to either an increase in v_s or a decrease in radius; Andrews *et al.* (2006) arrived to a similar conclusion by comparing their predictions of f_c and Q to real data. The added difficulty in measuring these modes stems from ${}_{11}S_2$ becoming an inner core confined mode through its 1-D cross-coupling to ${}_{10}S_2$, making it effectively unobservable and therefore providing insufficient data constraints to make a robust measurement of ${}_{11}S_2$. However, we do need to include ${}_{11}S_2$ in our measurements to accurately measure ${}_{10}S_2$ and their cross-coupling. So, mode ${}_{11}S_2$ is measured indirectly by its influence on mode ${}_{10}S_2$ and their cross-coupling. Table 1 shows our measured f_c and Q values calculated both with respect to PREM and the hybrid multiplet, together with the amount of data and misfits in the inversion.

Mode ${}_{10}S_2$ and its cross-coupling to ${}_{11}S_2$ exhibit anomalous zonal splitting, with strong zonal degree-two (c_{20}) and degree-four (c_{40}) values (Table 3). The typical zonal splitting is visible, with positive splitting anomalies located in the polar areas, and negative values around the equator (Fig. 3). The observed zonal splitting cannot be matched by mantle and crustal predictions, and is most easily explained by inner core cylindrical anisotropy with the fast axis aligned with the Earth's rotation axis (e.g. Woodhouse *et al.* 1986). However, none of the current inner core models can properly explain the observed anomalous splitting, they either overpredict the c_{20} and c_{40} values or even have the opposite expected sign (Table 3). ${}_{10}S_2$ is sensitive to the innermost inner core, which is not very well constrained by current anisotropy models. In addition, the fact that we observe anomalous zonal splitting in mode ${}_{10}S_2$, and specially in its cross-coupling to ${}_{11}S_2$, shows that cylindrical anisotropy needs to be present in the inner core, as these modes have little outer core and mantle sensitivity. Our ${}_{10}S_2$–${}_{11}S_2$ results contradict the suggestion that the origin of the anomalous zonal splitting is as likely to be present in the outer core as in the inner core (Romanowicz & Bréger 2000).

4.2 ${}_8S_2$–${}_9S_2$

We also measure the mode pair ${}_8S_2$–${}_9S_2$ (Table 1). The average Q values of the mode pair ${}_8S_2$–${}_9S_2$ are also affected by 1-D coupling (Figs 2c and d). However, unlike ${}_{10}S_2$–${}_{11}S_2$, this mode pair is not significantly affected by a small change in the 1-D model; their radial oscillations are invariant to these changes. Modes ${}_8S_2$–${}_9S_2$ are mostly sensitive to v_p (Fig. 2d), and our Q value measurements of ${}_8S_2$ and ${}_9S_2$ are much more similar to PREM predictions.

The splitting functions for modes ${}_8S_2$ and ${}_9S_2$ and their cross-coupling also show anomalous zonal splitting due to inner core cylindrical anisotropy (Figs 3d–f). These modes agree much better with current inner core model predictions than ${}_{10}S_2$–${}_{11}S_2$, because they sample the upper part of the inner core and are mainly sensitive to v_p, which is much better constrained by current inner core anisotropy models (Table 4).

5 DISCUSSION

5.1 Inner core radius and shear wave velocity

We compare our measured c_{00} splitting function coefficients for ${}_{10}S_2$ and ${}_{11}S_2$ with predictions for a range of inner core radius R and shear wave velocity v_s variations. We find that both a 2 per cent decrease in inner core radius R and a 2 per cent increase in v_s, like the one suggested by Andrews *et al.* (2006), are too great (Fig. 4). Because we include 3-D variations in our measurements due to inner core anisotropy, we need a smaller R decrease or v_s increase of only around 0.5 per cent. The c_{00} coefficients of both ${}_{10}S_2$ and the cross-coupling of ${}_{10}S_2$–${}_{11}S_2$ fall within a range of 0.5–0.75 per cent inner core R decrease or v_s increase, while the measurement of the less well constrained ${}_{11}S_2$, falls between 0.35 and 0.5 per cent R decrease or v_s increase.

To investigate if a small decrease in inner core radius or a small increase in inner core v_s would indeed be feasible, we tested the influence of increasing and decreasing R and v_s on other inner core sensitive modes. We restrict our comparison to modes dominated by inner core v_s using measurements of Deuss *et al.* (2013). We generate c_{00} predictions by varying PREM's inner core radius R and shear wave velocity v_s independently by up to 1 per cent; we have also applied a mantle and crust correction to the coefficients. Fig. 5 shows that most other v_s sensitive modes also agree with either a decrease in inner core radius or an increase in inner core v_s, in agreement with our observations for ${}_{10}S_2$–${}_{11}S_2$. It is not possible to distinguish between either a change in radius or inner core v_s, both fit the normal mode frequencies equally well.

Although in theory, our measured c_{00} splitting function coefficients can be due to a perturbation in any of the elastic parameters described in the 1-D model used (eq. 2), we consider the effect of 1-D changes in compressional velocity v_p and density ρ negligible. We find that neither an increase or a decrease in v_p can explain mode ${}_{10}S_2$ being visible, and only a disproportionate 40 per cent increase in inner core density is able to explain it.

If we assume that all contributions to the c_{00} coefficients come from an increase in inner core shear velocity, then our results do not agree with Tkalčić & Pham (2018), who measured an inner core v_s 2.5 per cent lower than PREM, using body wave observations of inner core shear waves travelling through the whole inner core. We would also disagree with Robson & Romanowicz (2019), who created a model that prefers an average inner core v_s 1 per cent lower than PREM. In their modelling they allowed v_s, v_p and ρ to change simultaneously and used 40 spheroidal modes mostly sensitive to the shallower inner core. However, we would agree with mineral physics studies of iron at high pressure and temperature, which usually find a v_s value 10–20 per cent larger than PREM (Vočadlo *et al.* 2003; Vočadlo 2007). Nonetheless, our proposed increase in v_s is still too small to explain the higher values from mineral physics. This effect was also explored by Deuss (2008), who showed through a synthetic normal mode study that the large v_s found in mineral physics cannot be reconciled with observations of inner core sensitive modes.

On the other hand, if we assume all contributions to the c_{00} coefficients come from an decrease in inner core radius, we would agree with de Wit *et al.* (2014), who found the inner core radius 0.1–0.3 per cent smaller than PREM. Like the studies mentioned in the

Table 3. Modes ${}_{10}S_2$–${}_{11}S_2$ predicted splitting function coefficients Re(c_{00}), Im(c_{00}), c_{20} and c_{40} for inner core and mantle models compared to our measurements, all in μHz. (∗) Indicates results are not well constrained. Numbers have been rounded-up for an easier comparison.

	${}_{10}S_2$				${}_{10}S_2$–${}_{11}S_2$				${}_{11}S_2$			
Model prediction	Re(c_{00})	Im(c_{00})	c_{20}	c_{40}	Re(c_{00})	Im(c_{00})	c_{20}	c_{40}	Re(c_{00})	Im(c_{00})	c_{20}	c_{40}
Woodhouse *et al.* (1986)	–	–	71	−44	–	–	−83	53	–	–	125	−67
Tromp (1993)	–	–	225	71	–	–	−283	−83	–	–	381	102
Durek & Romanowicz (1999)	–	–	1	−122	–	–	−21	138	–	–	63	−160
Beghein & Trampert (2003)	–	–	−28	23	–	–	−22	−25	–	–	121	24
S20RTS and CRUST5.1	−3	–	0.3	−0.2	−2	–	0.2	−0.2	−2	–	0.2	−0.1
+2 % IC v_s	112	–	–	–	−142	–	–	–	183	–	–	–
–2 % IC R	122	–	–	–	−148	–	–	–	175	–	–	–
Our measurements	40	−3	7	16	−40	−2	5	5	39*	−1*	8*	−2*

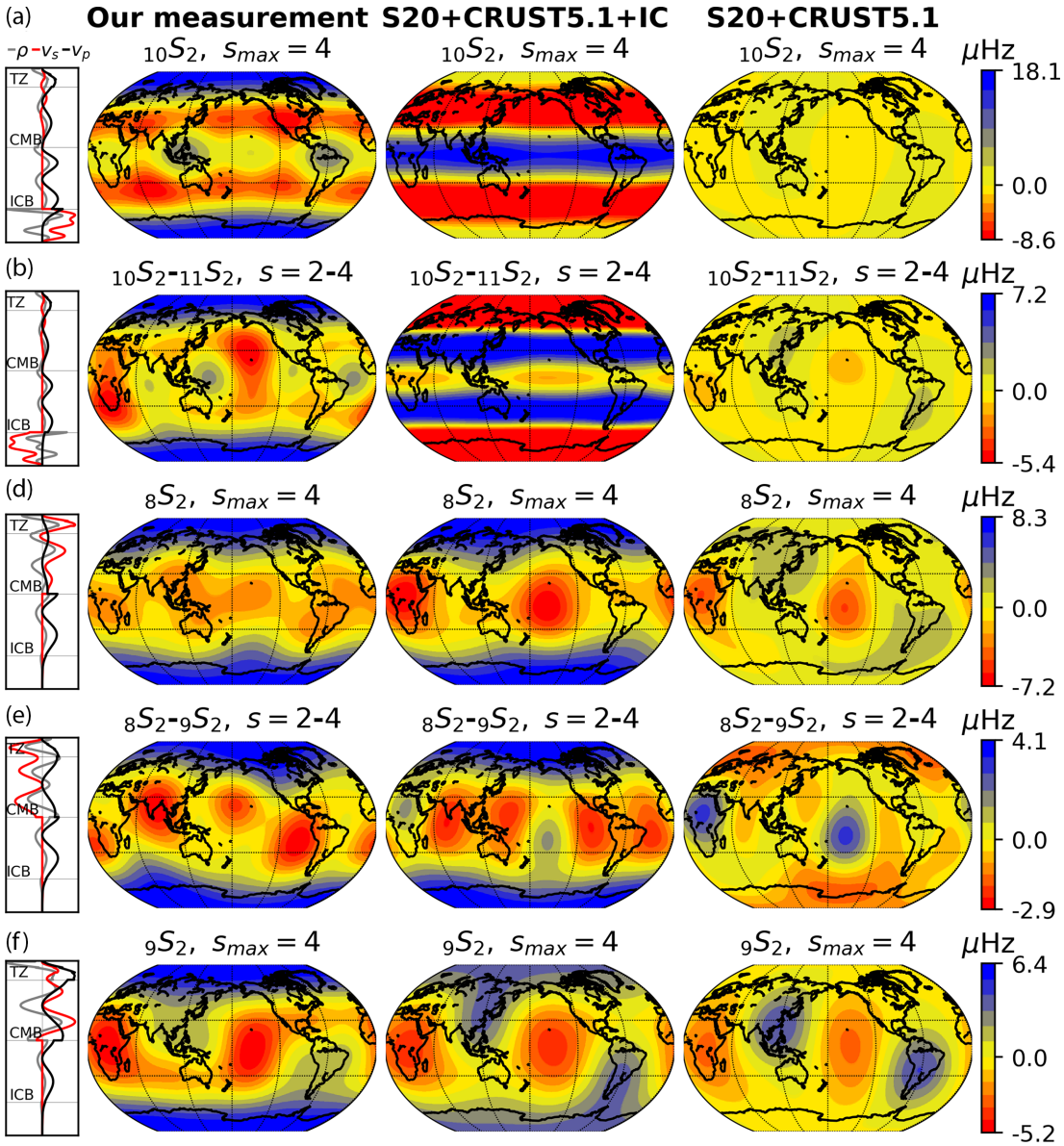

Figure 3. Self- and cross-coupling splitting functions measurements (left-hand panel) compared to a combined inner core, mantle and crustal model (middle panel) and a combined mantle and crustal model (right-hand panel). Corresponding sensitivity kernels and structural degree s are shown. Inner core model: Beghein & Trampert (2003), mantle model: S20RTS (Ritsema *et al.* 1999), crustal structure model: CRUST5.1 (Mooney *et al.* 1998).

previous paragraph, they also found the v_s of the shallow inner core ∼1 per cent smaller than PREM, although much less constrained than other parameters to be significant. They used 184 spheroidal modes to explore the trade-offs between v_p, v_s, ρ, Q_μ, Q_κ and depth discontinuities along the whole Earth radius.

Table 4. Modes ${}_8S_2$–${}_9S_2$ predicted splitting function coefficients Re(c_{00}), Im(c_{00}), c_{20} and c_{40} for inner core and mantle models compared to our measurements, all in μHz. Numbers have been rounded-up for an easier comparison.

	${}_8S_2$				${}_8S_2$–${}_9S_2$				${}_9S_2$			
Model prediction	Re(c_{00})	Im(c_{00})	c_{20}	c_{40}	Re(c_{00})	Im(c_{00})	c_{20}	c_{40}	Re(c_{00})	Im(c_{00})	c_{20}	c_{40}
Woodhouse *et al.* (1986)	–	–	3	−1	–	–	2	−1	–	–	2	−0.5
Tromp (1993)	–	–	7	2	–	–	5	1	–	–	3	1
Durek & Romanowicz (1999)	–	–	5	−0.5	–	–	3	−0.4	–	–	2	−0.3
Beghein & Trampert (2003)	–	–	9	2	–	–	6	1	–	–	4	1
S20RTS and CRUST5.1	−8	–	2	−0.5	4	–	−2	0	−8	–	0	0
+2% IC v_s	1	–	–	–	1	–	–	–	0.5	–	–	–
–2% IC R	−0.2	–	–	–	−0.1	–	–	–	−0.1	–	–	–
Our measurements	−1	4	9	2	−1	8	4	1	−3	−1	7	2

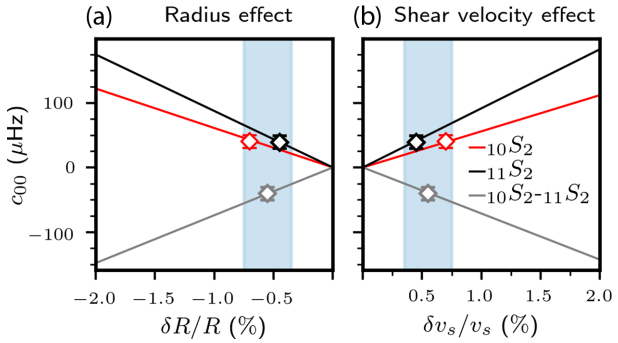

Figure 4. c_{00} coefficients as a function of (a) inner core radius $\delta R/R$ and (b) shear wave velocity $\delta v_s/v_s$, together with our measurements for modes ${}_{10}S_2$, ${}_{11}S_2$ and their cross-coupling. Blue area: (a) $-0.75\% < \delta R/R < -0.3\%$ and (b) $0.35\% < \delta v_s/v_s < 0.75\%$.

Here, for simplicity, we assume that our measured c_{00} values are affected either by inner core radius R or shear wave velocity v_s and not a combination. However, to be able to discern between the different contributions of these parameters, our ${}_{10}S_2$–${}_{11}S_2$ measurements should be used together with other inner core observations to create a model that is able to explain all of them. This has not been done yet, because mode ${}_{10}S_2$ has long been considered to be an outlier (Li *et al.* 1991; Widmer *et al.* 1991; Durek & Ekström 1996), both because of its high sensitivity to the underlying 1-D model used and the past measurements of its Q value. Here, we show that the source of ${}_{10}S_2$–${}_{11}S_2$ behaviour is the result of a perturbation to the 1-D elastic structure of the inner core, and not the 1-D anelastic structure.

5.2 Attenuation

We have shown that the high Q measured for ${}_{10}S_2$ is purely due to its strong 1-D Q cross-coupling to ${}_{11}S_2$, and not the result of a weakly attenuating inner core. The Q of ${}_{10}S_2$ is strongly dependent on changes to 1-D inner core shear wave velocity v_s and radius R, as well as cross-coupling due to inner core anisotropy and 1-D structure. Since 1-D coupling transforms these modes into a hybrid multiplet, we can no longer analyse their f_c and Q values with respect to PREM, as their sensitivity kernels and eigenfunctions have also changed. The hybrid multiplet generated has its own apparent f_c^h and Q^h, which we interpret as ${}_{10}S_2$ becoming more PKIKP equivalent and ${}_{11}S_2$ more inner core confined. However, these apparent values do not change the underlying $Q_\mu = 84$ of PREM, and should not be interpreted as evidence of a weakly attenuating inner core. Thus, our ${}_{10}S_2$–${}_{11}S_2$ measurements agree with the strongly attenuating inner core of PREM and suggests that strong inner core attenuation continues from body wave frequencies (e.g. Li & Cormier 2002), to the lower normal mode frequencies. Moreover, they are now in agreement with the other tested v_s sensitive inner core modes which also favour a strongly attenuating inner core.

Further tests were run using MINEOS (not shown) on the effect of the outer core's low attenuation on the f_c and Q of modes ${}_{10}S_2$ and ${}_{11}S_2$. We find that changing the Q_κ of the outer core has no significant effect on these modes, which means the resulting Q values must be attributed to the inner core. Unfortunately, we cannot specify a particular inner core depth range for our Q measurements, because of the very nature of splitting functions, which are depth weighted averages of how a mode 'sees' the Earth. We also do not distinguish between the inner core Q_μ and Q_κ observed by modes ${}_{10}S_2$ and ${}_{11}S_2$ because Q depends on both; although, like previous studies, we do expect both modes to be mostly influenced by Q_μ. In order to properly parametrize these variables, an inner core model inversion, that includes our ${}_{10}S_2$–${}_{11}S_2$ measurements and other normal mode data for a much larger number of inner core sensitive modes, should be performed.

In addition, to the ${}_{10}S_2$–${}_{11}S_2$ measurements reported in this study, we have also attempted to measure the 3-D elastic and anelastic structure of mode ${}_{10}S_2$ (Mäkinen & Deuss 2013). For this we performed four types of inversions (not shown): (i) measuring elastic and anelastic structure for ${}_{10}S_2$ on its own (ii) measuring elastic and anelastic structure only for ${}_{10}S_2$ with ${}_{11}S_2$ as predicted by PREM, and including cross-coupling through rotation and ellipticity, but no 1-D Q cross-coupling (iii) measuring elastic structure for ${}_{10}S_2$ and ${}_{11}S_2$ and all their cross-coupling, and measuring anelastic structure only for ${}_{10}S_2$ (iv) measuring elastic structure for ${}_{10}S_2$ and ${}_{11}S_2$ and all their cross-coupling, and measuring anelastic structure for ${}_{10}S_2$ and ${}_{11}S_2$. Cases (i) and (ii) produced large misfits (>0.9), even when using the measured elastic and anelastic splitting functions of Pachhai *et al.* (2020), who measured ${}_{10}S_2$ on its own, as a starting model. Cases (iii) and (iv) give similar results for the centre frequency and Q to the ones we obtain without including 3-D anelastic structure. Inversions (iii) and (iv) become unstable because of the larger number of parameters that are measured, and we don't consider them well constrained for publication. From these inversions we conclude 1-D Q coupling plays an essential role in fitting mode pair ${}_{10}S_2$–${}_{11}S_2$ to the real data. However, in the future, with the inclusion additional data, inversions for 3-D anelastic structure should be performed in combination with 1-D Q coupling.

5.3 Innermost inner core anisotropy

Current inner core models based on normal mode data (Woodhouse *et al.* 1986; Tromp 1993; Durek & Romanowicz 1999; Beghein &

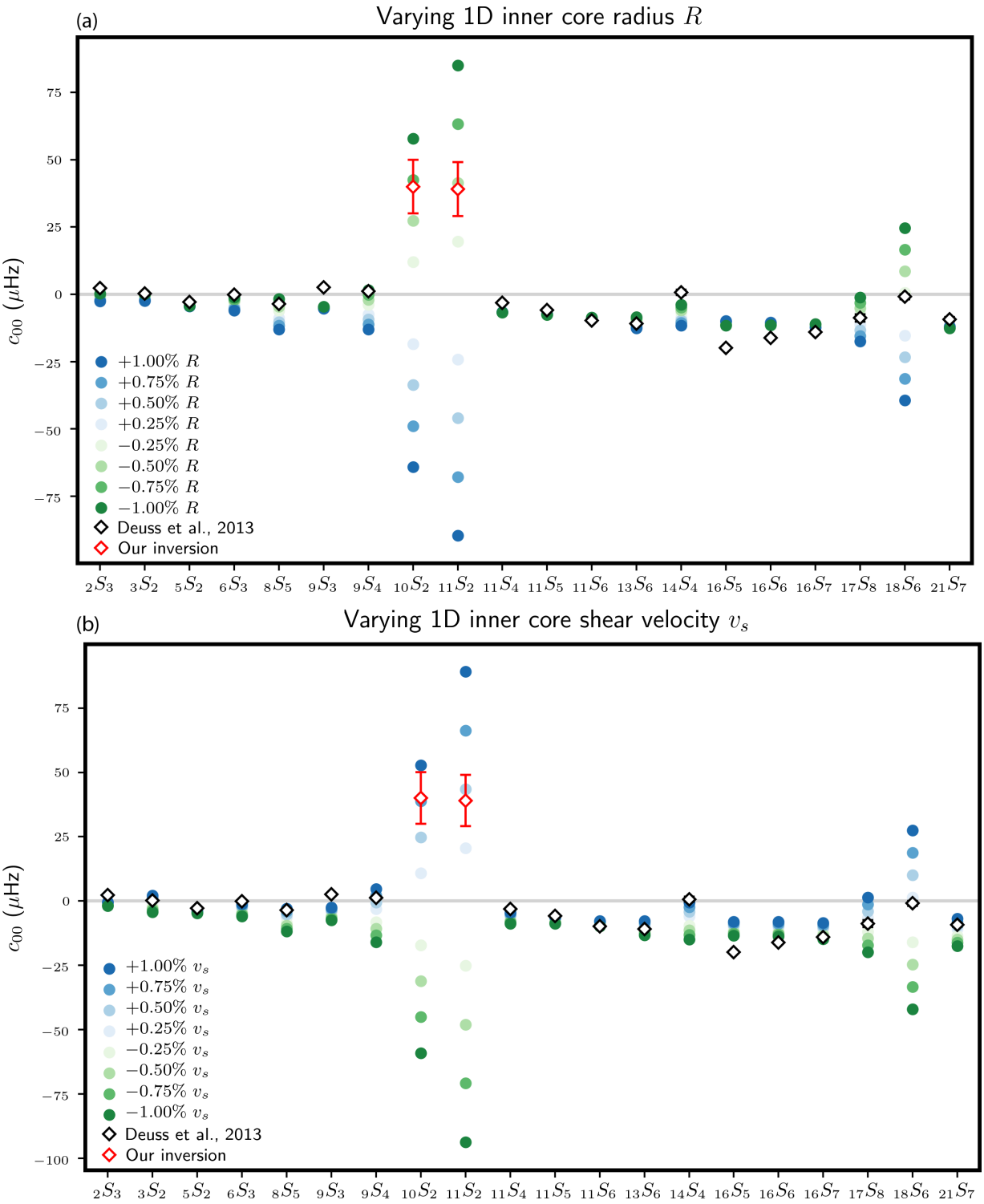

Figure 5. Predicted c_{00} coefficients for increasing and decreasing (a) inner core radius R and (b) shear velocity v_s, compared to Deuss *et al.* (2013) and our measurements.

Trampert 2003) predict contradictory c_{20} and c_{40} splitting function values for modes $_{10}S_2$, $_{11}S_2$ and their cross-coupling (Table 3). These models were built using modes mostly sensitive to the uppermost inner core with few exceptions (e.g. $_3S_2$). As a consequence, the seismic anisotropy parameters of these models differ significantly in the innermost 800 km of the inner core (Irving *et al.* 2008). Our measurements of $_{10}S_2$ and its cross-coupling to $_{11}S_2$ (Figs 3a and b) provide new constrains on anisotropy in the innermost inner core, which can be easily included in future inner core anisotropy modelling.

The predicted c_{20} and c_{40} values of the models are all much larger than our observed values, suggesting that current models overestimate the amount of anisotropy in the innermost inner core. One of the models, Beghein & Trampert (2003), predicts a negative c_{20}

value for ${}_{10}S_2$. We find that starting our inversions from negative c_{20} coefficients always leads to higher misfits (>0.42). This implies that our results contradict a flipping in the sign of inner core anisotropy in the lowermost inner core, as the one suggested by Beghein & Trampert (2003). In addition, although all inner core models predict a negative sign for the cross-coupling c_{20} coefficient, we find that the data is best fitted by a positive c_{20}, matching the sign of the mantle prediction.

6 CONCLUSIONS

We have measured modes ${}_{10}S_2$ and ${}_{11}S_2$ using perturbation theory including 1-D Q cross-coupling. We found that ${}_{10}S_2$ is the visible mode and that it is strongly split, while mode ${}_{11}S_2$ becomes completely inner core confined. Our observations are explained by either a 0.5 per cent increase in inner core v_s or a 0.5 per cent decrease in inner core radius, with respect to PREM, and the presence of inner core anisotropy. No change in Q_μ is needed, and our ${}_{10}S_2$–${}_{11}S_2$ observations are consistent with a strongly attenuating inner core with PREM values of $Q_\mu = 84$. Thus, unlike previously thought, a weakly attenuating inner core is not needed to explain observations of ${}_{10}S_2$–${}_{11}S_2$, in agreement with past measurements of other inner core sensitive modes.

ACKNOWLEDGEMENTS

We thank Vernon Cormier, Rudolf Widmer-Schnidrig and an anonymous reviewer for their constructive comments which helped to improve the manuscript. This project has received funding from the European Research Council (ERC) under the European Union's Horizon 2020 research and innovation programme (grant agreement No. 681535 - ATUNE) and a Vici award number 016.160.310/526 from the Netherlands organization for scientific research (NWO). The facilities of IRIS Data Services, and specifically the IRIS Data Management Centre, were used for access to waveforms, related metadata, and/or derived products used in this study. IRIS Data Services are funded through the Seismological Facilities for the Advancement of Geoscience (SAGE) Award of the National Science Foundation under Cooperative Support Agreement EAR-1851048. We also acknowledge the 'Global CMT project' webpage for the earthquake source parameters used in this study (Dziewonski *et al.* 1981; Ekström *et al.* 2012). The data analysis and figures were generated using Obspy (Beyreuther *et al.* 2010) and a Python package designed by Simon Schneider, Lisanne Jagt and STS.

REFERENCES

Andrews, J., Deuss, A. & Woodhouse, J., 2006. Coupled normal-mode sensitivity to inner-core shear velocity and attenuation, *Geophys. J. Int.,* **167**(1), 204–212, doi.org/10.1111/j.1365-246X.2006.03022.x.

Beghein, C. & Trampert, J., 2003. Robust normal mode constraints on inner-core anisotropy from model space search, *Science,* **299**(5606), 552–555, doi:10.1126/science.1078159.

Beyreuther, M., Barsch, R., Krischer, L., Megies, T., Behr, Y. & Wassermann, J., 2010. Obspy: a Python toolbox for seismology, *Seismol. Res. Lett.,* **81**(3), 530–533, doi.org/10.1785/gssrl.81.3.530.

Birch, A.F., 1940. The alpha-gamma transformation of iron at high pressures, and the problem of the Earth's magnetism, *Am. J. Sci.,* **238**(3), 192–211, doi: 10.2475/ajs.238.3.192.

Bullen, K., 1946. A hypothesis on compressibility at pressures of the order of a million atmospheres, *Nature,* **157**(3987), 405.

Cao, A., Romanowicz, B. & Takeuchi, N., 2005. An observation of PKJKP: inferences on inner core shear properties, *Science,* **308**(5727), 1453–1455, DOI: 10.1126/science.1109134.

Cormier, V.F., 1981. Short-period PKP phases and the anelastic mechanism of the inner core, *Phys. Earth planet. Inter.,* **24**(4), 291–301, doi.org/10.1016/0031-9201(81)90116-3.

Dahlen, F., 1968. The normal modes of a rotating, elliptical Earth, *Geophys. J. Int.,* **16**(4), 329–367, doi.org/10.1111/j.1365-246X.1968.tb00229.x.

Deuss, A., 2008. Normal mode constraints on shear and compressional wave velocity of the Earth's inner core, *Earth planet. Sci. Lett.,* **268**(3–4), 364–375, doi.org/10.1016/j.epsl.2008.01.029.

Deuss, A., Ritsema, J. & van Heijst, H., 2013. A new catalogue of normal-mode splitting function measurements up to 10 mHz, *Geophys. J. Int.,* **193**(2), 920–937, doi.org/10.1093/gji/ggt010.

Deuss, A. & Woodhouse, J.H., 2001. Theoretical free-oscillation spectra: the importance of wide band coupling, *Geophys. J. Int.,* **146**(3), 833–842, doi.org/10.1046/j.1365-246X.2001.00502.x.

Deuss, A., Woodhouse, J.H., Paulssen, H. & Trampert, J., 2000. The observation of inner core shear waves, *Geophys. J. Int.,* **142**(1), 67–73, doi.org/10.1046/j.1365-246x.2000.00147.x.

de Wit, R., Käufl, P., Valentine, A. & Trampert, J., 2014. Bayesian inversion of free oscillations for Earth's radial (an) elastic structure, *Phys. Earth planet. Inter.,* **237,** 1–17, doi.org/10.1016/j.pepi.2014.09.004.

Doornbos, D., 1983. Observable effects of the seismic absorption band in the Earth, *Geophys. J. Int.,* **75**(3), 693–711, doi.org/10.1111/j.1365-246X.1983.tb05006.x.

Durek, J.J. & Ekström, G., 1995. Evidence of bulk attenuation in the asthenosphere from recordings of the Bolivia Earthquake, *Geophys. Res. Lett.,* **22**(16), 2309–2312, doi.org/10.1029/95GL01434.

Durek, J.J. & Ekström, G., 1996. A radial model of anelasticity consistent with long-period surface-wave attenuation, *Bull. seism. Soc. Am.,* **86**(1A), 144–158.

Durek, J.J. & Romanowicz, B., 1999. Inner core anisotropy inferred by direct inversion of normal mode spectra, *Geophys. J. Int.,* **139**(3), 599–622, doi.org/10.1046/j.1365-246x.1999.00961.x.

Dziewonski, A. & Anderson, D., 1981. Preliminary reference earth model, *Phys. Earth planet. Inter.,* **25**(4), 297–356.

Dziewonski, A. & Gilbert, F., 1971. Solidity of the inner core of the Earth inferred from normal mode observations, *Nature,* **234**(5330), 465.

Dziewonski, A. & Gilbert, F., 1973. Observations of normal modes from 84 recordings of the Alaskan Earthquake of 1964 March 28th. Further remarks based on new spheroidal overtone data, *Geophys. J. Int.,* **35**(4), 401–437.

Dziewonski, A.M., Chou, T.-A. & Woodhouse, J.H., 1981. Determination of earthquake source parameters from waveform data for studies of global and regional seismicity, *J. Geophys. Res.,* **86,** 2825–2852.

Edmonds, A.R., 1960. *Angular Momentum in Quantum Mechanics,* Princeton Univ. Press.

Ekström, G., Nettles, M. & Dziewonski, A.M., 2012. The global CMT project 2004-2010: Centroid-moment tensors for 13,017 earthquakes, *Phys. Earth Planet. Inter.,* **1-9,** 200–201.

Giardini, D., Li, X.-D. & Woodhouse, J.H., 1988. Splitting functions of long-period normal modes of the Earth, *J. geophys. Res.,* **93**(B11), 13 716–13 742.

Gilbert, F., 1971. The diagonal sum rule and averaged eigenfrequencies, *Geophys. J. Int.,* **23**(1), 119–123.

He, X. & Tromp, J., 1996. Normal-mode constraints on the structure of the Earth, *J. geophys. Res.,* **101**(B9), 20 053–20 082.

Irving, J., Deuss, A. & Andrews, J., 2008. Wide-band coupling of Earth's normal modes due to anisotropic inner core structure, *Geophys. J. Int.,* **174**(3), 919–929.

Koelemeijer, P., Deuss, A. & Ritsema, J., 2013. Observations of core-mantle boundary Stoneley modes, *Geophys. Res. Lett.,* **40**(11), 2557–2561.

Lehmann, I., 1936. P', publ, *Bur. Centr. Seism. Internat. Serie A,* **14,** 87–115.

Li, X. & Cormier, V.F., 2002. Frequency-dependent seismic attenuation in the inner core, 1. A viscoelastic interpretation, *J. geophys. Res.,* **107**(B12), ESE–13.

Li, X.-D., Giardini, D. & Woodhouses, J.H., 1991. Large-scale three-dimensional even-degree structure of the Earth from splitting of long-period normal modes, *J. geophys. Res.,* **96**(B1), 551–577.

Masters, G. & Gilbert, F., 1981. Structure of the inner core inferred from observations of its spheroidal shear modes, *Geophys. Res. Lett.,* **8**(6), 569–571.

Masters, G. & Gilbert, F., 1983. Attenuation in the Earth at low frequencies, *Phil. Trans. R. Soc. Lond., A,* **308**(1504), 479–522.

Masters, G. & Shearer, P., 1990. Summary of seismological constraints on the structure of the Earth's core, *J. geophys. Res.,* **95**(B13), 21 691–21 695.

Mooney, W., Laske, G. & Masters, G., 1998. CRUST5.1: a global model at 5 degrees by 5 degrees, *J. geophys. Res,* **102,** 727–748.

Morozov, I.B., 2015. On the relation between bulk and shear seismic dissipation, *Bull. seism. Soc. Am.,* **105**(6), 3180–3188.

Mäkinen, A.M. & Deuss, A., 2013. Normal mode splitting function measurements of anelasticity and attenuation in the Earth's inner core, *Geophys. J. Int.,* **194**(1), 401–416.

Pachhai, S., Masters, G. & Laske, G., 2020. Probabilistic estimation of structure coefficients and their uncertainties, for inner-core sensitive modes, using matrix autoregression, *Geophys. J. Int,* **221**(2), 1366–1383.

Resovsky, J. & Ritzwoller, M., 1998. New and refined constraints on three-dimensional Earth structure from normal modes below 3 mHz, *J. geophys. Res.,* **103**(B1), 783–810.

Resovsky, J., Trampert, J. & Van der Hilst, R., 2005. Error bars for the global seismic Q profile, *Earth planet. Sci. Lett.,* **230**(3), 413–423.

Ritsema, J., van Heijst, H.J. & Woodhouse, J.H., 1999. Complex shear wave velocity structure imaged beneath Africa and Iceland, *Science,* **286**(5446), 1925–1928.

Ritzwoller, M., Masters, G. & Gilbert, F., 1986. Observations of anomalous splitting and their interpretation in terms of aspherical structure, *J. geophys. Res.,* **91**(B10), 10 203–10 228.

Robson, A.J. & Romanowicz, B., 2019. New normal mode constraints on bulk inner core velocities and density, *Phys. Earth planet. Inter.,* **295,** doi.

Romanowicz, B. & Bréger, L., 2000. Anomalous splitting of free oscillations: a reevaluation of possible interpretations, *J. geophys. Res.,* **105**(B9), 21 559–21 578.

Romanowicz, B. & Mitchell, B., 2007. Deep Earth structure: Q of the Earth from crust to core, in *Treatise on Geophysics,* 2nd edn, pp. 731–774, Schubert, G., Elsevier.

Tarantola, A. & Valette, B., 1982. Generalized nonlinear inverse problems solved using the least squares criterion, *Rev. Geophys.,* **20**(2), 219–232.

Tkalčić, H. & Pham, T.-S., 2018. Shear properties of Earth's inner core constrained by a detection of J waves in global correlation wavefield, *Science,* **362**(6412), 329–332.

Tromp, J., 1993. Support for anisotropy of the Earth's inner core from free oscillations, *Nature,* **366**(6456), 678.

Vočadlo, L., 2007. Ab initio calculations of the elasticity of iron and iron alloys at inner core conditions: evidence for a partially molten inner core?, *Earth planet. Sci. Lett.,* **254**(1–2), 227–232.

Vočadlo, L., Alfè, D., Gillan, M., Wood, I., Brodholt, J. & Price, G.D., 2003. Possible thermal and chemical stabilization of body-centred-cubic iron in the earth's core, *Nature,* **424**(6948), 536.

Widmer, R., 2002. Non-linear constraints for 1-D elastic core structure from the attenuation of $_{10}S_2$, in *Annual DGG Meeting Abstracts*.

Widmer, R., Masters, G. & Gilbert, F., 1991. Spherically symmetric attenuation within the Earth from normal mode data, *Geophys. J. Int.,* **104**(3), 541–553.

Woodhouse, J., 1980. The coupling and attenuation of nearly resonant multiplets in the Earth's free oscillation spectrum, *Geophys. J. Int.,* **61**(2), 261–283.

Woodhouse, J., 1988. The calculation of the eigenfrequencies and eigenfunctions of the free oscillations of the earth and sun, *Seismological Algorithms, Computational Methods and Computer Programs,* pp. 321–370, Doornbos, D. J., Academic Press.

Woodhouse, J. & Dahlen, F., 1978. The effect of a general aspherical perturbation on the free oscillations of the Earth, *Geophys. J. Int.,* **53**(2), 335–354.

Woodhouse, J. & Giardini, D., 1985. Inversion for the splitting function of isolated low order normal mode multiplets, *EOS Trans. Am. Geophys. Un.,* **66,** 300.

Woodhouse, J., Giardini, D. & Li, X.-D., 1986. Evidence for inner core anisotropy from free oscillations, *Geophys. Res. Lett.,* **13**(13), 1549–1552.

Wookey, J. & Helffrich, G., 2008. Inner-core shear-wave anisotropy and texture from an observation of PKJKP waves, *Nature,* **454**(7206), 873.